

**ADVANCED  
MATERIALS**  
INTERFACES

Supporting Information

for *Adv. Mater. Interfaces.*, DOI: 10.1002/admi.201600501

Peptide–Polymer Conjugates for Bioinspired  
Compatibilization of Internal Composite Interfaces: via  
Specific Interactions toward Stiffer and Tougher Materials

*Valeria Samsoninkova, Britta Seidt, Felix Hanßke, Wolfgang  
Wagermaier, and Hans G. Börner\**

## Supporting Information

### **Peptide-polymer conjugates for bio-inspired compatibilization of internal composite interfaces: Via specific interactions toward stiffer and tougher materials**

*Valeria Samsoninkova, Britta Seidt, Felix Hanßke, Wolfgang Wagermaier, Hans G. Börner\**

To whom correspondence should be addressed:

Prof. Dr. Hans G. Börner

Humboldt-Universität zu Berlin; Chemistry Department

Laboratory for Organic Synthesis of functional Systems

12489 Berlin, Germany

E-Mail: [h.boerner@hu-berlin.de](mailto:h.boerner@hu-berlin.de)

## Materials and Methods

### Materials

#### For conjugate synthesis

Sidechain-protected L-amino acids Fmoc-Gly-OH, Fmoc-Thr(*t*Bu)-OH, Fmoc-Gln(Trt)-OH, Fmoc-Tyr(*t*Bu)-OH, Fmoc-Ala-OH, Fmoc-Ser(*t*Bu)-OH, Fmoc-Lys(Boc)-OH, Bromotrimethylsilane (TMSBr), *N*-methyl-2-pyrrolidone (NMP, 99.9+%, peptide synthesis grade), 2-(1H-benzotriazole-1-yl)-1,1,3,3-tetramethyluronium hexafluorophosphate (HBTU), 1-Hydroxybenzotriazole (HOBt), dichloromethane (DCM, peptide grade), used for peptide synthesis, were purchased by IRIS Biotech (Marktredwitz, Germany). NMP was filtrated before use, DCM was distilled, other chemicals were used as received.

*N,N*-diisopropylethylamine (DIPEA, peptide grade), piperidine (peptide grade), Trifluoroacetic acid (TFA, peptide grade), 2,5-dihydroxybenzoic acid (DHB) (MALDI MS matrix) were purchased by Acros Organics (Thermo Fisher Scientific) (Watham, MA, USA). Guanidinium chloride (99.5%) was obtained from Carl Roth (Karlsruhe, Germany). TentaGel® PAP resin (PEG attached peptide resin, loading: 0.24 mmol g<sup>-1</sup>; M<sub>n</sub> = 3200) was obtained from Rapp Polymere (Tübingen, Germany).

DMSO d<sub>6</sub> with 99,9% purity was obtained in ampules from Deutero GmbH (Kastellen, Germany).

#### For composites preparation

PEO, used as a matrix with M<sub>n</sub>=900.000, PEG for reference experiments with M<sub>n</sub>= 3000; methanol (≥99.6%) and magnesium turnings (99.98%) for magnesium fluoride synthesis were obtained from Sigma Aldrich (St. Louis, U.S.A). Hydrogen fluoride (>99%) was obtained from Solvay Fluor (Hannover, Germany)) and used as methanolic solution. Methanol (LC-MS grade) was bought from Acros Organics.

## Equipment

### For composite preparation and characterization

**Hot pressing:** Hot pressing of the composite materials was performed on the SPECAC machines from Specac Limited (Orington, UK) at a constant temperature of 70°C. First the composites are heated without load for 3 min, then 1 ton of pressure is applied for 1 min, followed by 2 tons of pressure for 3 min. The composites are cooled down in the special cooling device with circulating water for 2 min. To prevent sticking of the composite to the pressing plates and to ensure quick release from the pressing plates, Polyethylene terephthalate (PET) foil is used. The average thickness of the composite ranges from 80-120  $\mu\text{m}$ . The thickness of the composite can be varied using different rings.

**Tensile testing:** The tensile testing experiments are realized in the small tensile stage with the stretching speed 5  $\mu\text{m/s}$ . The system allows very precise measurement of displacement via videoextentiometry.

For the evaluation of the tensile toughness, the same kind of samples was tested on the Zwick machine with testing speed 200 mm/min.

The modulus is calculated as the initial slope of the stress strain curve, and the energy to failure is calculated as the area under the stress-strain curve. The stress is calculated as the engineering stress, or maximum force divided by initial effective cross-sectional area. The correction for the true stress was not done, due to very different behavior of the composites depending on the concentration and not applicability of the correction to all curves. 8 samples were tested per concentration in each type of experiment. Samples showed very high sensitivity to the defects especially for energy to failure experiments.

**Electron microscopy:** Transmission electron microscopy (TEM) measurements were performed on the Philips CM200 (Eindhoven, Netherlands) operating at 200 keV accelerating voltage in bright field (BF) mode. Specimens for imaging by TEM were prepared by

evaporating a droplet of composite solution consisting of polymer, conjugate and nanoparticles sol onto carbon coated copper grid.

Electron microscopy pictures were done on the Jeol LEO 1550 (Oberkochen, Germany) with acceleration voltage 9 keV in BSE (backscattered electron) mode. The samples were sputtered with Pt/Pd before measurement.

**FT-IR:** Attenuated total reflection Fourier-Transform-Infrared Spectroscopy (ATR FTIR) analysis was performed on a FT-IR spectrometer Vertex 70 from Bruker Optik GmbH (Leipzig Germany) with diamond ATR crystal with the resolution of  $4\text{ cm}^{-1}$ . Conjugate was measured in a solid state and solid composites were investigated after hot pressing. All the samples were measured in vacuum.

**X-Ray diffraction (XRD):** Diffraction patterns were obtained with a Bruker D8 from Bruker AXS (Karlsruhe, Germany) device with Cu K $\alpha$  ( $\lambda=1.5418\text{ \AA}$ ) radiation equipped with a scintillator detector to determine the grade of crystallinity. The data evaluation was performed by using the software program EVA. The degree of crystallinity of a polymer can be investigated by comparing the area under the crystalline peaks to the total scattered intensity.

**SAXS:** Small-angle X-ray scattering (SAXS) experiments using synchrotron radiation were performed at the  $\mu$ Spot Beamline at the Bessy II (Helmholtz Zentrum Berlin Adlershof, Germany). The 2 dimensional diffraction patterns were recorded with a 2D CCD detector MarMosaic 225 from Rayonix Inc (Evanston, U.S.A.) with a pixel size of  $73\text{ }\mu\text{m}$  and an array of  $3072 \times 3072$  pixels.

To carry out the calibrations of sample-to-detector distance and beam center, a quartz standard and the software Fit2D (ESRF, v. 12.077) were used. For the acquisition of the 2D pattern, the energy of the X-Ray beam ( $100\text{ }\mu\text{m}$  in diameter; wavelength,  $\lambda = 0.82656\text{ \AA}$ ) of 15keV and a sample-to-detector distance of 300 mm were calibrated. All patterns were first

corrected for empty beam background scattering, radially averaged to obtain the function  $I(q)$  and intensity corrected. The data evaluation was performed using the software package DPDAK (DESY/MPIKG, Gunthard Benecke and Chenghao Li, v. 1.2) and OriginPro. The spectra were obtained in the  $q$ -range of 0.3 to 8 nm<sup>-1</sup>.

### **For conjugate synthesis and characterization**

**Conjugate synthesis:** Solid-phase peptide synthesis (SPPS) was done with an ABI 433A peptide synthesizer by Applied Biosystems (Darmstadt, Germany).

**Mass spectrometry (MS):** Mass spectrometry was done by Bruker autoflex III smartbeam with matrix assisted laser desorption/ionization (MALDI) and time of flight detector (MALDI-ToF-MS) (Rheinstetten, Germany). For MALDI-MS the samples were dissolved in water, while the matrix was dissolved in water/acetonitrile/TFA (1:1:0.1%, v/v/v). Matrix and sample solutions were mixed directly on the plate in a ratio of 2:1. It was measured in linear positive mode.

**Nuclear Magnetic Resonance (NMR) Spectroscopy:** <sup>1</sup>H NMR spectrum was measured on Bruker AVANCE II 500. NMR samples were dissolved in DMSO d<sub>6</sub> 99,8%.

## Methods

**MgF<sub>2</sub> synthesis:** The synthesis of MgF<sub>2</sub> was performed under inert atmosphere (Ar) using Schlenk techniques. Mg turnings (2.43 g, 100 mmol) were dissolved in 500 mL dried methanol to yield Mg(OMe)<sub>2</sub> at a concentration of 0.2 M. To initiate fluorolysis a stoichiometric amount of HF dissolved in methanol was slowly added under vigorous stirring to give the desired product. Aging for 2-3 weeks resulted in optically clear sols. <sup>19</sup>F NMR (300 MHz, locked in CDCl<sub>3</sub> in methanol,  $\delta$ ): -154 (BF<sub>4</sub><sup>-</sup> from reaction of HF with glass vessel), -187 (HF<sub>adsorbed</sub>), -198 ppm (MgF<sub>2</sub>).

**Solid-phase supported peptide synthesis (SPPS):** Peptide-PEO conjugates were synthesized according to standard Fmoc procedures with side-chain protected amino acids (AA). ABI-Fastmoc protocols (single coupling for 1st to 10th AA, double coupling afterwards, capping; *N*-terminal acetylation followed in NMP using TentaGel® PAP resin. AA coupling was facilitated by HBTU/DIPEA. After final deprotection the resin was washed thoroughly with NMP and DCM. The cleavage was done with TFA/TMSBr/Thioanisol = 94:1:5 (v/v/v) for 2 x 1 h. The conjugates were precipitated in cold diethyl ether and centrifuged. The dried conjugates were dissolved in water with guanidine hydrochloride (0.1% w/v). Conjugates are then dialyzed against Milli-Q® water for ca. 4 days with change of solvent at least three times per day.

**Preparation of composites:** the preparation procedure of the composites consisted of two steps: solution casting and hot pressing. An appropriate amount of the peptide-polymer conjugate was dissolved in methanol (LC-MS grade), after which a certain amount of MgF<sub>2</sub> sol was added. The mixture was stirred for a minimum of 4 hours to allow the conjugate to adhere to the inorganic surface. A 5 wt% aqueous solution of PEO (900 kg mol<sup>-1</sup>) was added and all components were mixed for another 30 min. The total volume of the prepared solution was 5 ml. The solution was cast into a small bowl and the material was dried under an

extraction hood for 12 hours. The material that was obtained after the solution casting step was not suitable for the mechanical testing experiments, which require even and homogeneously thick composites. A hot pressing procedure was applied to prepare composite materials in order to eliminate unevenness in thickness of composites. With an average thickness of 80-120  $\mu\text{m}$ , samples were cut in a typical bone form with a length of 18 mm and a width of 6 mm.

### Analysis of conjugate

#### Mass spectrometry

Ac-GTQYYAYSTTQKS-PEG

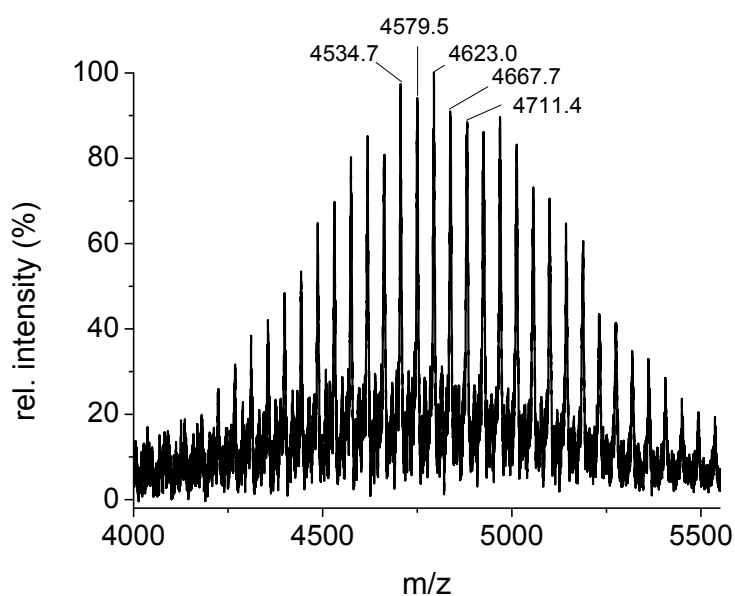


**Figure S1.** MALDI-ToF-MS of conjugate.

MS (MALDI-ToF)  $m/z$ :  $[M + H]^+$  calc, 4579.06 Da; found, 4579.56 Da; calculated with 69 EO units.

$[M + Na]^+$  calc, 4601.06 Da; found, 4601.35 Da; (the underlying peak)

$\Delta m = 44.05$   $m/z$ , characteristic for repeating ethylene oxide (EO) units;

The mass can be assigned within  $\pm 0.5$   $m/z$  accuracy.

**NMR**

Ac-Gly-Thr-Gln-Tyr-Tyr-Ala-Tyr-Ser-Thr-Thr-Gln-Lys-Ser-PEG

(Ac-G<sub>1</sub>T<sub>2</sub>Q<sub>3</sub>Y<sub>4</sub>Y<sub>5</sub>A<sub>6</sub>Y<sub>7</sub>S<sub>8</sub>T<sub>9</sub>T<sub>10</sub>Q<sub>11</sub>K<sub>12</sub>S<sub>13</sub>-PEG)

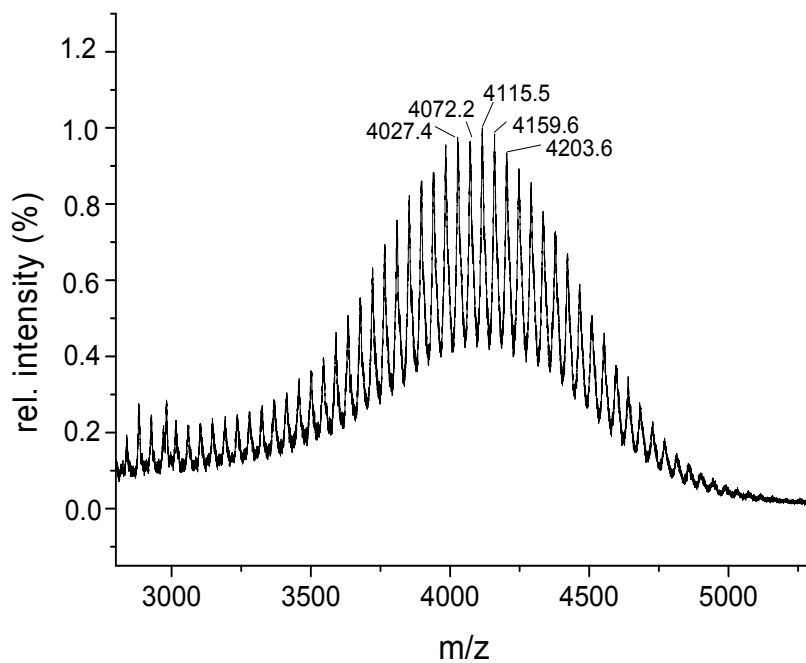
<sup>1</sup>H NMR (500 MHz, [D<sub>6</sub>] DMSO, 25 °C, TMS): 0.97 ppm (d, 3 H; γCH<sub>3</sub> T<sub>2</sub>), 1.02-1.10 ppm (t, 6 H; γCH<sub>3</sub> T<sub>9</sub>, T<sub>10</sub>), 1.17 ppm (d, 2 H; γ, δCH<sub>2</sub> K<sub>12</sub>), 1.28-1.37 ppm (m, 3 H; γ, δ CH<sub>2</sub> K<sub>12</sub>), 1.72-1.65 ppm (m, 2 H; βH A<sub>6</sub>, δCH<sub>2</sub> K<sub>12</sub>), 1.94-1.72 ppm (m, 4 H; βH Q<sub>3</sub>, G<sub>11</sub>), 1.98-2.18 ppm (m, 4 H; γH Q<sub>3</sub>, G<sub>11</sub>), 2.56-2.98 ppm (m, 8 H; βH + CH S<sub>8</sub>, Y<sub>4</sub>; Y<sub>5</sub>, Y<sub>7</sub>), 3.21 ppm (m, 2 H; βH S<sub>13</sub>), 3.51 ppm (m, 326 H; CH<sub>2</sub> PEG), 3.59 ppm (m, 1 H; βH S<sub>8</sub>), 3.63-3.67 ppm (m, 3 H; βCH Y<sub>4</sub>; Y<sub>5</sub>, Y<sub>7</sub>), 3.78 ppm (m, 1 H; αH G<sub>1</sub>), 3.97 ppm (m, 1 H; βH T<sub>2</sub>), 4.01-4.12 ppm (m, 2 H; βH T<sub>9</sub>, T<sub>10</sub>), 4.37-4.15 ppm (m, 9 H; αH T<sub>2</sub> Q<sub>3</sub> Q<sub>11</sub> A<sub>6</sub> T<sub>10</sub> K<sub>12</sub> S<sub>13</sub> Y<sub>4</sub> T<sub>9</sub>), 4.39-4.46 ppm (m, 2 H; αH Y<sub>5</sub> S<sub>8</sub>), 4.50 ppm (m, 1 H; αH Y<sub>7</sub>), 4.89 – 4.98 ppm (t, d, d, 3 H; OH S<sub>13</sub>, T<sub>9</sub>, T<sub>10</sub>), 5.03- 5.14 ppm (t, d, 2 H; OH S<sub>8</sub> T<sub>2</sub>) 6.58-6.66 ppm (q, s, 6 H; εH CH Y<sub>4</sub> Y<sub>5</sub> Y<sub>7</sub>), 6.76-6.83 ppm (d, 2 H; δNH<sub>2</sub> Q<sub>3</sub> Q<sub>11</sub>), 6.92-6.98 ppm (d, 2 H; δCH Y<sub>4</sub>), 6.99-7.05 ppm (q, 4 H; δCH Y<sub>5</sub> Y<sub>7</sub>), 7.22-7.29 ppm (d, 2 H; δNH<sub>2</sub> Q<sub>3</sub> Q<sub>11</sub>), 8.21—8.13 ppm (m, 2 H; NH G<sub>1</sub> S<sub>8</sub>), 8.07-7.94 ppm (m, 5 H; NH K<sub>12</sub>, A<sub>6</sub> Q<sub>3</sub> Q<sub>11</sub> Y<sub>5</sub>), 7.79-7.71 ppm (d, 3 H; NH Y<sub>7</sub> T<sub>10</sub> T<sub>2</sub>), 7.94-7.81 ppm (m, 6 H; NH S<sub>13</sub> T<sub>9</sub> Y<sub>4</sub>; 1H; εNH<sup>3+</sup> K<sub>12</sub>; 2 H; δNH<sub>2</sub> Q<sub>3</sub> Q<sub>11</sub>)

**IR spectroscopy**

ATR-IR:  $\nu = 3283 \text{ cm}^{-1}$  (m; Amid A);  $2890 \text{ cm}^{-1}$  (w, C-H);  $1624 \text{ cm}^{-1}$ ;  $1665 \text{ cm}^{-1}$ ;  $1697 \text{ cm}^{-1}$  (s, Amid I);  $1518 \text{ cm}^{-1}$  (m, Amid II);  $1467 \text{ cm}^{-1}$  (m),  $1343 \text{ cm}^{-1}$  (m);  $1280 \text{ cm}^{-1}$  (m);  $1241 \text{ cm}^{-1}$  (m);  $1203 \text{ cm}^{-1}$  (w, Amide III);  $1145 \text{ cm}^{-1}$  (w);  $1104 \text{ cm}^{-1}$  (s);  $1062 \text{ cm}^{-1}$  (w);  $962 \text{ cm}^{-1}$  (m);  $842 \text{ cm}^{-1}$  (m);  $722 \text{ cm}^{-1}$  (vw, Amide IV).

Gly-Ala-Lys-Thr-Ser-Tyr-Thr-Tyr-Gln-Ser-Thr-Tyr-Gln-PEG

(GAKTSYTYQSTYQ-PEG)

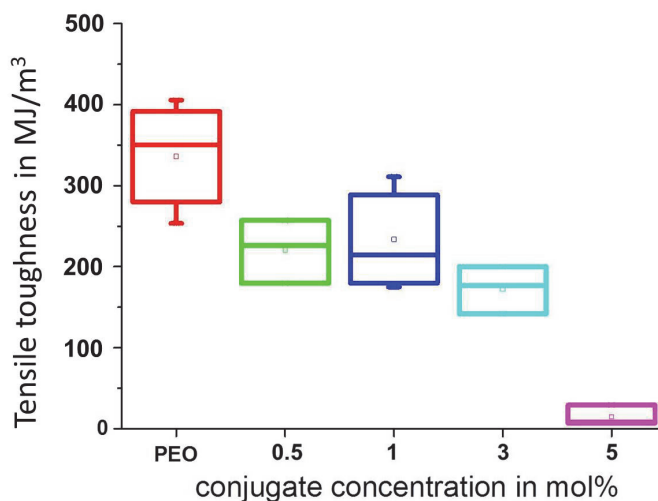


**Figure S2.** MALDI-ToF-MS of scrambled conjugate.

MS (MALDI-ToF)  $m/z$ :  $[M + Na]^+$  calc, 4115.6 Da; found, 4115.5 Da; calculated with 59 EO units.

$\Delta m = 44$  m/z, characteristic for repeating ethylene oxide (EO) units;

The mass can be assigned within  $\pm 0.1$  m/z accuracy.

**Mechanical testing****Impact of the conjugate addition on the matrix**

**Figure S3.** Pure conjugate without inorganic filler added to PEO matrix decrease of tensile toughness and increasing brittleness of composite with the raising conjugate concentration.

Pure conjugate without addition of inorganic filler was added to the system to evaluate the impact of the conjugates on the matrix. Tensile toughness was calculated for various concentrations from 0.5-5 mol%. Overall pure conjugate present in the matrix has a negative impact on it, lowering the values of toughness. The conjugate concentrations of 0.5-3 mol% cause similar changes; further increase of concentration to 5 mol% makes the material very brittle and reduces toughness dramatically. This observation can be explained by the self-assembly issues taking place with the increasing conjugate concentration.

### Role of peptide-particle interaction

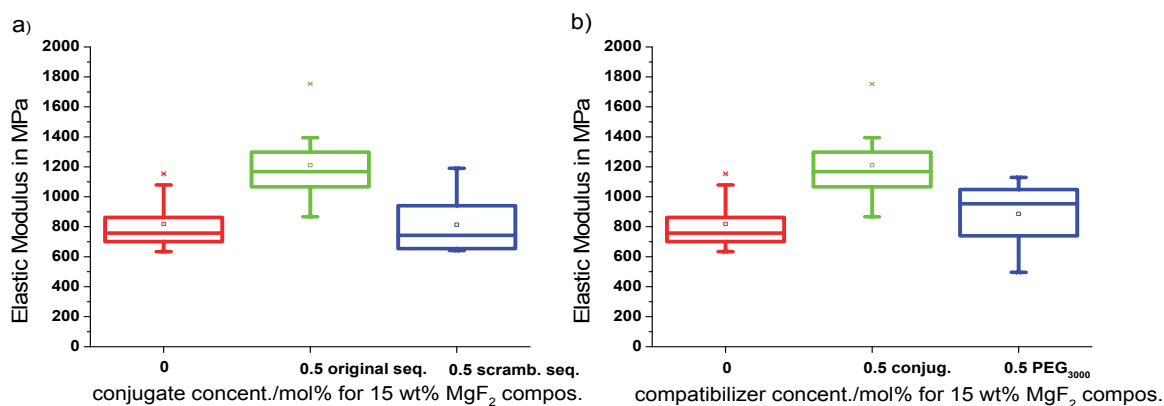


**Figure S4.** Control experiments realized on the example of 15wt% MgF<sub>2</sub> filled composites: a. Incorporated in a conjugate scrambled peptide sequence used instead of original one does not lead to higher elastic modulus values compared to non-stabilized composites, indicating the sequence specificity of binding. b. PEG<sub>3000</sub> used as a compatibilizer was not able to stabilize the particle and increase the elastic modulus values evidencing the requirement of the peptide in the compatibilizer.

Two types of experiments were performed to evaluate the importance of peptide-particle interaction. All experiments were realized on the example of 15wt% MgF<sub>2</sub> filled composites. In one experiment the original sequence was scrambled, meaning that the same amino acids were placed in a different order. In another experiment peptide segment was removed from the conjugate and just PEG<sub>3000</sub> was used for compatibilization. For both experiments influence of these peptide-particle interactions was evaluated on the example of elastic modulus.

Change of the peptide sequence leads to the lowering of mechanical performance. The same effect is observed if the peptide segment is removed from the system. These two experiments clearly show that the interaction between peptides and the inorganic component is the main reason for the improvement of mechanical properties.

### Particle-size distribution in the composites

Samples with 15 wt% MgF<sub>2</sub> filling were investigated in HR-SEM in back-scattered

electron (BSE) Modus to evaluate size and distribution of the particles in the composites. Backscattered electrons were detected in order to distinguish the particles from the matrix. In comparison to the secondary electrons, backscattered electrons are sensitive to the different elemental composition and penetrate more deeply into the sample, providing the information not only about the surface.  $\text{MgF}_2$  particles will appear as the bright spots. Electron microscopy pictures were done with acceleration voltage 9 keV, which was revealed as the optimal accelerating voltage for these samples. Lower voltage level did not eject enough backscattered electrons to generate sufficient contrast. As a drawback of quite high voltage level, samples can be quickly damaged during measurement leading to cracks visible in micrographs.

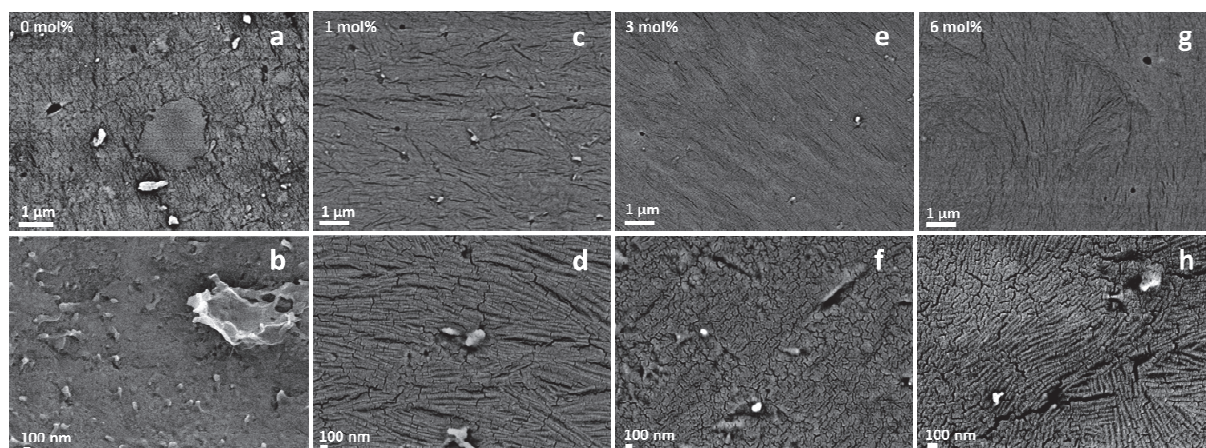


**Figure S5.** Suppression of particle agglomeration in the 15 wt%  $\text{MgF}_2$  filled composites with stepwise increase of conjugate concentration: a,b - 0 mol%, c,d - 1 mol%, e,f - 3 mol%, g,h - 6 mol% in SEM (BSE) micrographs.

SEM micrographs reveal the transition in the sizes of filler depending on the conjugate concentration.  $\text{MgF}_2$  particles added to the matrix from the sol with the particle size of 2 nm agglomerate severally and cause formation of agglomerates in the  $\mu\text{m}$  range visible on SEM micrographs. This process is naturally occurring and based on the tendency of very small particles with high surface area and high energy to reduce it by agglomeration. Each portion of conjugate added to the system reduces the size of formed agglomerates and  $\mu\text{m}$  agglomerates disappear, moving to submicron and nm particles (agglomerates). Particles in

the highly stabilized composites can be only found with higher magnification. This study clearly evidences the size transition, but it does not provide quantitative information about the sizes of filler in the composites with different conjugate concentration. To eliminate this gap, particle-size distribution diagrams were generated based on the scanning electron microscopy study.

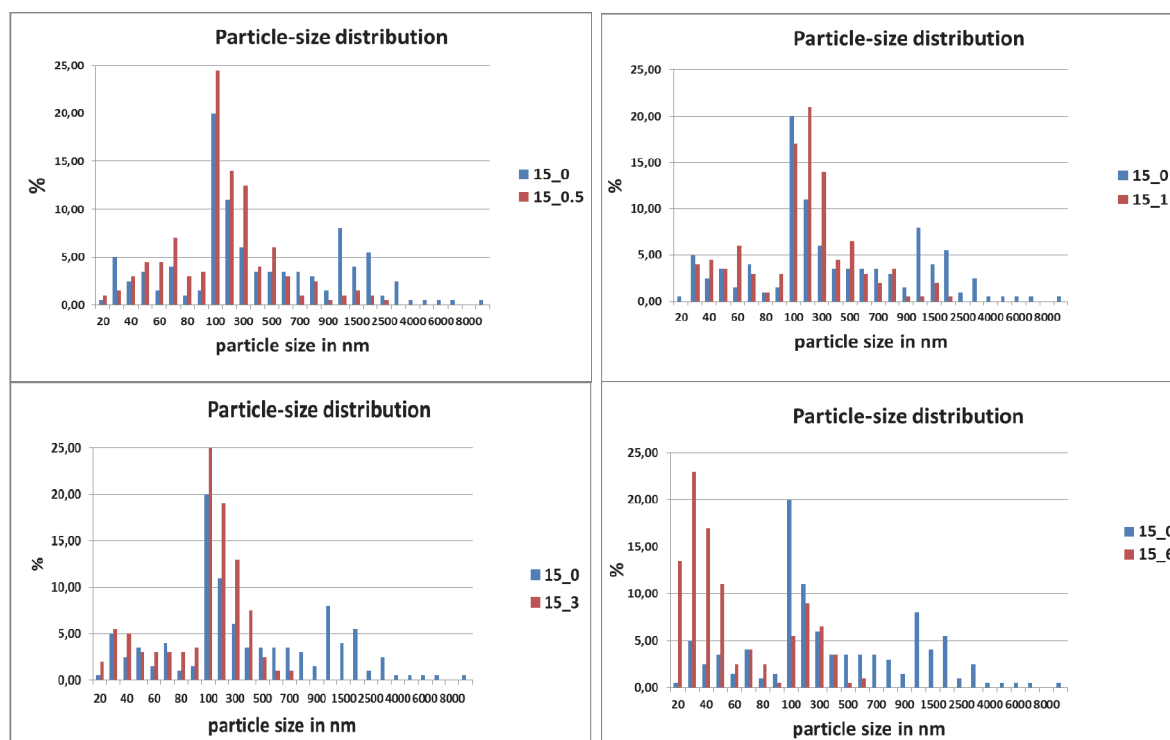


**Figure S6.** Particle-size distribution for 15wt% MgF<sub>2</sub> filled composites with 0;1;3;6 mol% conjugate concentration indicates decrease of filler size and narrowing the distribution with rising conjugate concentration.

The statistics is built on the base of 200 particles randomly selected per each sample. The size of the particles was measured with Image J program. First the scale bar on the picture is measured to determine how many pixels it represents. Then the objects on the micrograph are measured. Knowing how many pixels object on the micrograph and scale bar contain, solving the proportion, the size of objects can be calculated in nm. It should be noted that this procedure does not consider the particles below 10 -20 nm due to limits in resolution of the method.

Particle-size distribution diagrams provide more detailed information about the average

sizes of particles in composites with different conjugate concentration. Composites without addition of conjugate have a combination of agglomerates of various sizes ranging from  $\mu\text{m}$  agglomerates to nm particles with domination of submicron aggregation of 100-300 nm in sizes. Firstly, addition of 0.5 mol% conjugate prevent only formation of bigger agglomerates (bigger than 3  $\mu\text{m}$ ) keeping nm and submicron aggregates unchanged. Further addition of conjugate lead to more narrow particle-size distribution and in the case of 3 mol% all measured particles are smaller than 1  $\mu\text{m}$ . In the case of 6 mol% bigger agglomerates disappear and around 80% of the particles are below 100 nm. From these observations it becomes clear that stepwise addition of the conjugate to the system leads to better stabilization of nanoparticles and step by step decreases aggregate sizes. One should note that conjugates cannot stabilize the particles to the full extent and keep them the same as in sol in the range of 2 nm.

**SAXS data evaluation**

To calculate radius  $R$  of the  $\text{MgF}_2$  nanoparticles the data were fitted by following Emmerling et al. using the Equation 1.:<sup>1</sup>

$$I(q) = I_0B + I_0 [V_0 S(q)P(q)] \quad (1)$$

Where  $V_0$  is the mean volume of the particles,  $P(q)$  is their form factor and  $S(q)$  is the structure factor describing the packing of the primary particles.<sup>2</sup>  $I_0$  is a normalization constant depending on the set-up and  $B$  is a constant background from the sample<sup>[1]</sup>. By assuming nearly spherical particles with a radius  $R$  the volume of the particles can be defined as follow (Equation 2):<sup>3</sup>

$$V_0 = 4\pi R^3/3 \quad (2)$$

For the form and structure factor (Equation 3 and 4) for this system we can take:

$$P(q) = 1 / [1 + \sqrt{2} (qR)^2 / 3]^2 \quad (3)$$

$$S(q) = 1 + C(D)/(qR)^D \quad (4)$$

$D$  is the fractal dimension and  $C(D)$  is a constant depending on  $D$ <sup>[2]</sup> (Equation 5):

$$C(D) = D\Gamma(D - 1)\sin[\pi(D - 1)/2] \quad (5)$$

**Table S1.** Increase of radius of  $\text{MgF}_2$  particles in the composites with raising conjugate concentration detected by SAXS.

Sample	R [nm]
PEO + 15% $\text{MgF}_2$	0.98±0.01
PEO + 15% $\text{MgF}_2$ + 0.5 mol% conjugate	1.03±0.01
PEO + 15% $\text{MgF}_2$ + 1 mol% conjugate	1.13±0.01
PEO + 15% $\text{MgF}_2$ + 2 mol% conjugate	1.35±0.02
PEO + 15% $\text{MgF}_2$ + 3 mol% conjugate	1.36±0.06
PEO + 15% $\text{MgF}_2$ + 6 mol% conjugate	1.41±0.01

The constant  $B$  was nearly the same for all samples (in the order of  $0.007 \text{ nm}^3$ ). As this parameter cannot easily be described and is also negligible for the contribution  $q < 0.2 \text{ nm}^{-1}$  we won't discuss it in detail. The determined radii  $R$  for all samples are summarized in Tab. 1.

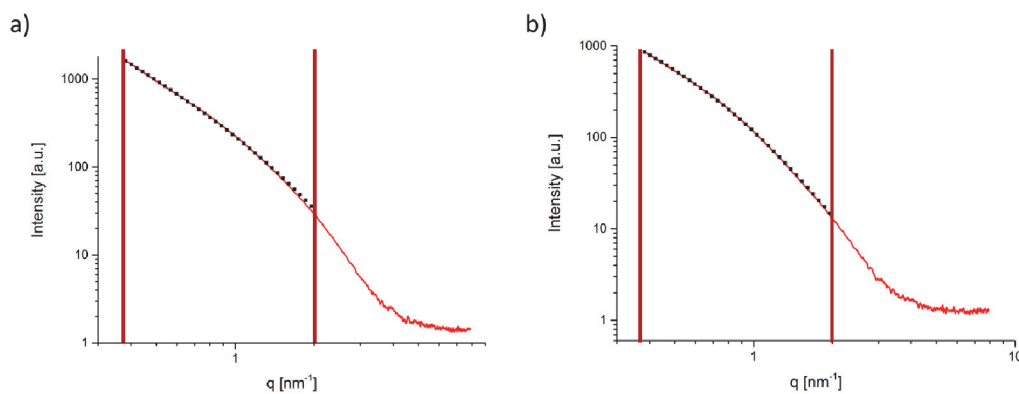


**Figure S7.** SAXS intensity as a function of the scattering vector  $q$  for selected sample compositions with a) PEO + 15% MgF<sub>2</sub> and b) PEO + 15% MgF<sub>2</sub> + 6 mol% conjugate. The red lines show the experimental data and the black dots show the fits used to determine particle radius.

Scattering curves of selected samples are shown in Figure S7. The fit was performed in the range between  $0.3 \leq q \leq 2.0 \text{ nm}^{-1}$  as we are interested only in the radius  $R$ , the contribution of polydispersity to the system was negligible. An Anova one-way analysis suggests that all samples and values for radius  $R$  are significantly different.

## Self-assembly and agglomeration of conjugates

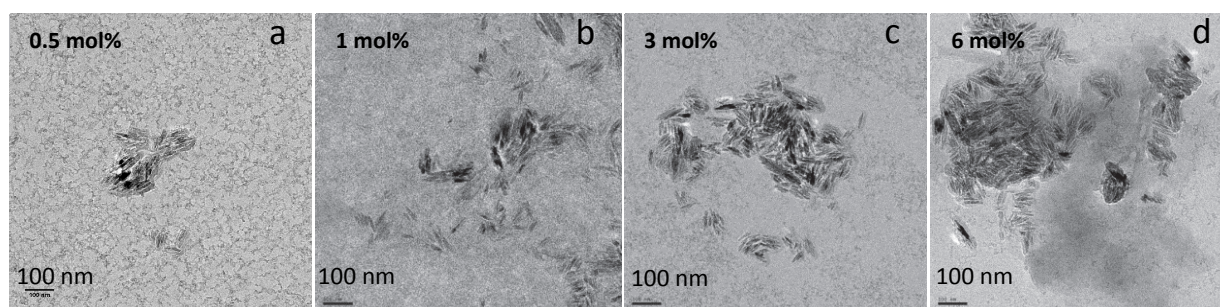


**Figure S8.** TEM micrographs evidence rod like structures formed as a result of self-assembly of conjugates using the example of 15wt% MgF<sub>2</sub> composites with 0,5;1;3;6 mol% conjugates (a-d) Rods are assembled in agglomerates, which increase in size with raising concentration.

TEM studies of materials reveal the formation of rod-like structures. AFM and TEM studies of pure conjugates evidence the same structures of the same size. The increase of conjugate concentration stimulates the assembly of the rods forming agglomerates. The size of formed structures increases with the rising concentration. But all TEM micrographs indicate formation of structures of increased size reaching 500 nm – to 1  $\mu$ m in case of 6 mol%. It becomes clear that starting from 3 mol% of conjugates, the agglomerates reach the size of  $\mu$ m and start to introduce a negative impact on the polymer matrix, exactly when the toughness starts to decrease. This allows us to conclude that the structures make material more brittle.

<sup>1</sup>A. Emmerling, R. Petricevic, A. Beck, P. Wang, H. Scheller, J. Fricke, J. Non-Cryst. Solids **1995**, 185, 240.

<sup>2</sup>N. Husing, U. Schubert, K. Misof, P. Fratzl, *Chem. Mater.* **1998**, 10, 3024.

<sup>3</sup>J. Noack, L. Schmidt, H. J. Glasel, M. Bauer, E. Kemnitz, *Nanoscale* **2011**, 3, 4774.